Agricultural Water Management 283 (2023) 108301

Contents lists available at ScienceDirect

Agricultural Water Management

journal homepage: www.elsevier.com/locate/agwat

Visualization of uncertain leaching fraction and drought exposure as a function of irrigation dosage and frequency

F.D. Mondaca-Duarte[a,*], D. Reyes-Lastiri[a], M. Heinen[b], E.J. van Henten[a], S. van Mourik[a]

[a] Wageningen University, Farm Technology Group, P.O. Box 16, 6700 AH Wageningen, the Netherlands
[b] Wageningen Environmental Research, Wageningen UR, P.O. Box 47, 6700 AA Wageningen, the Netherlands

ARTICLE INFO

Handling Editor: Dr Z Xiying

Keywords:
Performance framework
Model-based irrigation
Drought exposure
Leaching fraction
Monte Carlo
Decision support

ABSTRACT

There is a need for precise irrigation strategies to reduce leaching and water use, whilst avoiding drought exposure. A model-based prediction and visualization method is proposed to help estimate the precise required irrigation dosage and frequency to achieve desired leaching fraction and drought exposure as a multi-objective optimization problem. The method produces a contour plot that shows the estimated leaching and drought exposure under uncertain evapotranspiration. Three sandy soils and three clay soils were examined for a total of 6 different soils, which included a clay soil case with protected Chrysanthemum cultivation. The results illustrate the usefulness of this type of visualization in decision support. Predictions indicate that compared to a conventional irrigation strategy, leaching could be reduced by 40% and water use by 9% whilst maintaining a low drought exposure (below 1%). Furthermore, predictions indicate that reducing evapotranspiration uncertainty would require an irrigation frequency increase (~20%) or a total irrigation dosage increase (~10%). Compared to clay soils, sandy soils require a higher frequency irrigation (more than once per 2 days) to prevent drought exposure. The proposed model-based framework and visualization method provides a useful understanding of low-risk irrigation strategies that account for evapotranspiration uncertainty, while reducing water use and minimizing leaching, giving valuable insights to agricultural professionals and policymakers alike. Additionally, the developed framework has the potential to be used as a core for decision and control tools developed for sustainable agriculture and water resource management.

1. Introduction

Given the current growth in world population, the need to maintain a steady level of food production is increasing the agricultural use of resources, including freshwater. Agriculture is the largest single user of freshwater, accounting for nearly 75% of current human freshwater use (FAO, 2016). A considerable share (45%) of that water is used for irrigation. A crucial aspect in achieving ecological sustainability in farming is to achieve an optimal irrigation balance.

1.1. Irrigation balance

Over-irrigation is an important cause of water waste. In addition to contributing to high water use, it also causes percolation within the soil. This may cause nutrients and biocides to be transported into the groundwater, causing a negative environmental impact (Erisman et al., 2011). It is therefore imperative to minimize over-irrigation. Irrigating too little, of course, is unwanted as this will lead to drought stress. At the same time, however, the complete elimination of percolation would lead to soil salinity, a potential source of crop stress.

The main cause of over-irrigation stems from misperceptions on the part of growers regarding the amount of water required (Levidow et al., 2014). From the grower's perspective, maximum crop production levels are desirable. The risk of yield loss due to drought conditions is always present and hard to foresee. Growers therefore tend to use over-irrigation as a form of risk avoidance, thereby protecting their crops from drought exposure (Perry et al., 2009). In contrast, from an environmental perspective, an important objective is to reduce water use as well as soil percolation emissions.

In addition to these objectives, high soil salinity should be avoided. The reduction of soil percolation to near-zero values may result in a build-up of solutes that are present due to fertilization or fertigation. A proportion of the built-up solutes is leached out from the root zone to prevent crop stress. The fraction of applied water that passes and

* Corresponding author.
E-mail address: francisco.mondacaduarte@wur.nl (F.D. Mondaca-Duarte).

https://doi.org/10.1016/j.agwat.2023.108301
Received 22 September 2021; Received in revised form 28 March 2023; Accepted 31 March 2023
Available online 7 April 2023

percolates throughout the entire rooting depth is known as the leaching fraction (LF) (Ayers et al., 1985).

Finding a balance between the aforementioned objectives requires precise irrigation scheduling regarding timing and dosage (Morison et al., 2008). The optimization of irrigation through precise timing and dosage is a form of ‘precision farming’, a strategy for resource-efficient food production that involves precise dosage, timing, and allocation of inputs, including nutrients and water (van Mourik et al., 2021). Their study illustrates precision farming with a model-based irrigation strategy with respect to water dosage and irrigation frequency. Many studies have been conducted on the improvement of irrigation frequency and dosage, based on both experimental and model-based approaches.

1.2. Experimental studies

Experimental studies have determined the effects of varying irrigation frequency and dosage on yield production by exploring crop-water demand due to evapotranspiration. These studies also indicate how irrigation strategies based on evapotranspiration can help to increase crop yield and reduce water use.

Studies by (Ertek et al., 2004; Sensoy et al., 2007) considered the effects of irrigation frequency and dosage on the production rate of field-grown melon and summer squash, concluding that the combination of higher irrigation frequency together with higher irrigation dosage increased yield whilst maintaining the soil water content above the wilting point.

In a study of the yield and quality of cucumber crops, (Abd El-Mageed et al., 2018) conclude that irrigation can be reduced from 100% to 80% of the evapotranspiration demand of the crop, with no major effect on yield, whilst reducing the amount of irrigation water applied by 20%.

These experimental studies demonstrate that tuning of dosage and frequency can result in considerable improvement in water-use efficiency without negatively affecting crop quality or production.

1.3. Model-based and uncertainty

Model-based studies allow fast and extensive exploration of irrigation strategies in a structural fashion, thereby offering the possibility to save time and labour input required for experimental studies. Computational analysis makes it possible to obtain insight into how variation in certain factors (e.g., soil type, crop type, and weather) may influence performance in terms of soil percolation and water use.

A study of Aggarwal (Aggarwal, 1995) focused on the influence of prediction uncertainty in e.g., weather and crop status on yield output. In that study, input uncertainty resulted in uncertain grain yield (with a standard deviation of 15%), evapotranspiration (with a standard deviation of 5%) and nitrogen uptake (with a standard deviation of 3%). These results suggest that uncertainty in input and parameters can have a considerable effect on model predictions. Nevertheless, model-based studies have not yet devoted much attention to the effect of parameter uncertainty in model predictions.

The incorporation of uncertainty analysis in model-based studies offers significant advantages over traditional experimental studies. By exploring irrigation strategies in a structural fashion, computational analysis allows for extensive and rapid exploration of different scenarios, thus saving time and resources. However, the inherent prediction uncertainty of soil-crop-weather systems poses a challenge to model-based studies. Variability in weather and soil properties can significantly impact model predictions, resulting in uncertain outcomes. This is why the study of Mondaca et al. (Mondaca-Duarte et al., 2020a, 2020b) applied a model-based approach to predict the relation between soil percolation and drought exposure under variable dosage, and under uncertainty in evapotranspiration rate and soil properties. The irrigation frequency was fixed (one irrigation per three days). For their test case they concluded that it is possible to reduce soil percolation by 88% and water use by 22% compared to a conventional irrigation strategy, whilst maintaining a low risk of crop stress due to drought exposure (< 1%). Their approach of incorporating uncertainty in evapotranspiration rate and soil properties in their model predictions of soil percolation and drought exposure is a novel and important approach to address these issues. However, one of the limitations of the study is that the optimal irrigation strategy shown applies to a specific case with a fixed irrigation frequency. In reality, this becomes an optimization problem as a feasible strategy will vary depending on the growers objective and capabilities. Further research is needed to account for the influence and interactions of various external factors.

1.4. The optimization problem

Finding the optimal balance between drought exposure, water-use and leaching poses an interesting optimization problem. Standard optimization strategies aim to identify an optimal solution amongst a set of feasible solutions by minimizing a cost function that balances objectives such as minimizing water use, maintaining a small but nonzero leaching fraction, and achieving an acceptably small drought exposure. The solution of the optimization problem depends on the relative weights assigned to each objective. Selecting the weights is not a straightforward procedure, as their associated objectives are hard to compare due to their different nature (ecological sustainability versus production rate). It is generally unclear how leaching or water use are to be weighed against drought exposure, as they depend on a variety of variable factors, e.g., related to government policies, risk avoidance of growers, market prices, delivery contracts, water availability, crop resilience to drought, natural soil salinity, and local climate.

The presence of multiple objectives usually creates a set of optimal solutions, instead of a single optimal solution. A way to visualize multi-objective optimization involves Pareto-optimal solutions (Sarkar and Modak, 2005). These solutions typically form an isoline along which the objective function is constant, thereby visualizing the trade-off between multiple conflicting objectives. Pareto optimization has been applied in real-life scheduling scenarios (Delgoda et al., 2017) or parameter optimization through inverse modelling (Vrugt et al., 2008).

When optimization of agricultural irrigation strategies is considered, it is also a complex problem that requires balancing multiple conflicting objectives such as water use, leaching fraction, and drought exposure. Selecting the relative weights of these objectives is not straightforward and depends on a variety of factors. The application of a multi-objective optimization to balance these objectives is a novel approach that has not yet been applied to direct agricultural irrigation strategies. The closest example is the study of (Udias et al., 2018) where a multi-objective optimization approach was used in irrigation dosage based on land use and soil slope characteristics. However, no studies have yet been published that use multi-objective optimization to balance water use, drought exposure, and soil percolation. This highlights the importance of incorporating optimization techniques that allow for the identification of the optimal solution amongst a set of feasible solutions while visualizing the trade-off between multiple conflicting objectives. Therefore, incorporating these optimization techniques is a novel approach that can significantly contribute to the optimization of agricultural irrigation strategies.

1.5. Objective

The objective of this study was to propose and illustrate a method for gaining insight into the combined effect of the time between irrigation (frequency) and total irrigation values (dosage) on leaching and drought exposure predictions under uncertain environmental conditions. This method visualises performance isolines of leaching and drought exposure as a function of the control variables irrigation dosage and frequency.

The method was applied to the case of (soil-based) Chrysanthemum cultivation in a greenhouse. The case study focused on the following four questions. The first question concerns the extent to which water use and leaching can be reduced by modifying the dosage and frequency of irrigation on a specific type of soil. The second question concerns the effect of including uncertainty in evapotranspiration on predictions of leaching, and drought exposure. The third question concerns how water use, and leaching relate to the frequency and dosage of irrigation, given a specific allowed drought exposure ratio. The fourth question concerns how the variation within and between soils affect drought exposure and leaching fraction as function of irrigation dosage and frequency.

The materials and methods used to investigate these questions are described in Section 2, and the results are presented in Section 3 including a discussion/reflection on both the results and the methodology. Section 4 presents conclusions for each question and recommendations for further research.

2. Materials and methods

The methodology used in this study can be summarized in the following steps.

1. A two-module model framework (Mondaca-Duarte et al., 2020b) was used to generate predictions of soil percolation and drought exposure (Section 2.1).
2. The model framework was extended to enable varying irrigation frequencies (Section 2.2).
3. A performance matrix was created for each type of soil. This matrix was used to compare predictions of drought exposure and leaching ratio based on different irrigation frequencies (x-axis) and irrigation dosages (y-axis). Outputs of the matrix were the leaching fraction ratio and drought exposure ratio (Section 2.3).
4. A Monte Carlo random sampling approach was used to simulate daily evapotranspiration uncertainty (Section 2.4).
5. Given the noise in the outputs of the performance matrix due to deviations in radiation inputs, the data values were smoothed using a moving-average algorithm (Section 2.5).
6. The smoothed irrigation matrices were plotted, including the frequency and dosage of irrigation and predictions of the drought exposure ratios and leaching fraction ratios (Section 2.6).
7. The smoothed irrigation matrices were analysed in view of the research questions (Sections 2.6 and 2.7).

2.1. Model description

The model used in this study is a continuation of a previous study by (Mondaca-Duarte et al., 2020b) involving the development of a two-module framework based on two models. In that study, the EMMAN3G model, which is based on the FUSSIM2D (Heinen, 2001) model, was used to describe a one-dimensional vertical water transport through three soil layers (0–30 cm, 30–60 cm, 60–90 cm), and the De Graaf model (Voogt et al., 2000) was used to calculate the evapotranspiration required by the EMMAN3G model for crop-water uptake

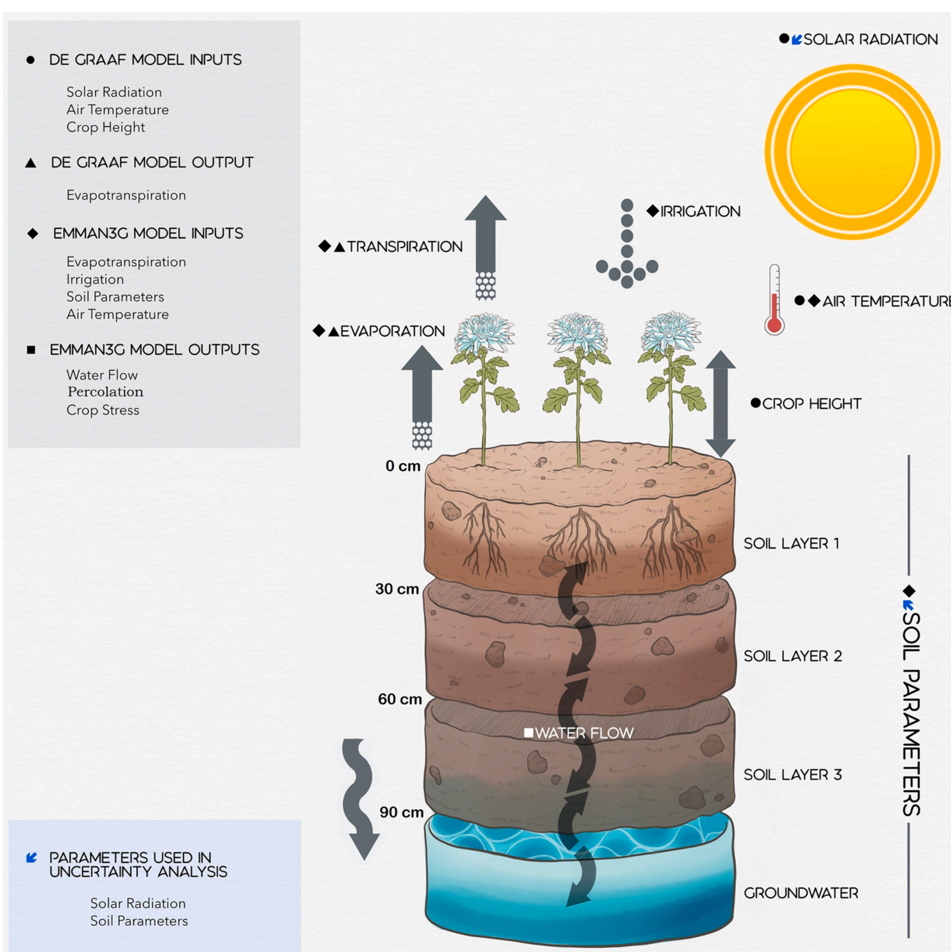

Fig. 1. Graphic description of the two-module model, graphical abstract modified from (Mondaca-Duarte et al., 2020a).

(Fig. 1).

In the De Graaf model, evapotranspiration is a function of global radiation, greenhouse temperature, heating-pipe temperature, and crop stage. The two-module framework has been verified and validated by (Mondaca-Duarte et al., 2020b), and full descriptions of the equations and methodology used to integrate the models are available in that publication.

In this study, soil percolation is defined as the amount of water leaving the soil at the bottom of the soil layer 3 towards groundwater. Total irrigation is defined as the total amount of water used by an irrigation strategy. Frequency relates to the amount of time between irrigation events. Water flow from the first soil layer can occur in two ways; through water flow to the second layer and through evapotranspiration. Drought exposure is the ratio of hours during which a crop root zone (first soil layer) is exposed to conditions below a water pressure head threshold below which transpiration reduction occurs resulting in decreased crop growth.

2.2. Model-based analysis

The period for the model-based analysis consisted of 32 consecutive days, starting on July 31st 2016. This period is the same as the experimental data period previously used in (Mondaca-Duarte et al., 2020b), during this period the crop is considered fully grown, for this reason the soil evaporation was neglected.

The De Graaf model focuses on the relationship between transpiration, evapotranspiration, and the radiation that the crop receives. Although soil evaporation can contribute to the overall evapotranspiration, for fully grown crops, it is usually possible to disregard it and concentrate only on transpiration. This is because transpiration accounts for the majority of the ET process for mature crops (Liebhard et al., 2022; Wei et al., 2017).

The model-based analysis focused on the two-module framework to predict drought exposure and leaching fraction, based on the dosage and frequency of irrigation. Irrigation dosages ranged between 103 mm and 173 mm, with a step size of 1 mm, resulting in 71 different irrigation dosages, which are listed along the y-axis of a matrix. Each irrigation dosage represents the accumulated irrigation used during the whole 32 days period. This means that as the frequency goes down, the amount that is administrated at each instance will increase, and vice versa.

The dosage irrigation values (y-axis) are based on the cumulative evapotranspiration from the De Graaf model, as calculated with the experimental data. The lower limit corresponds to 90% of the cumulative evapotranspiration, with the upper limit of irrigation corresponding to 150% of the cumulative evapotranspiration (114 mm). The lower limit was selected based on the conclusion of (Mondaca-Duarte et al., 2020b) that a decrease in dosage to near and lower than the cumulative evapotranspiration increased drought exposure exponentially. In the same manner, the upper limit of 150% cumulative evapotranspiration is based on the finding that irrigation values above this cumulative evapotranspiration range had near-zero drought exposure.

The time between irrigation events (displayed along the x-axis) were based on possible irrigation schedules. The lower limit is once an hour, and the upper limit is once every 168 h, corresponding to an irrigation event once every seven days. There were thus 168 different frequency values.

The resulting performance matrix of 71 irrigation values and 168 frequency values yielded a total of 11,928 unique combinations. For each of these combinations the model predicted a leaching fraction and a drought exposure.

2.3. Leaching fraction and drought exposure predictions

In the model soil percolation is represented as the downward water flow from the third soil layer, as it assumes that the groundwater table is just below the third soil layer. Total soil percolation was defined as the cumulative soil percolation over the total range of time-series data. The leaching fraction was defined as the sum of soil percolation divided by the irrigation,

$$LF = \frac{\sum Sp_i}{\sum I_i} \tag{1}$$

where LF [mm mm^{-1}] is the leaching fraction, Sp [mm] is the soil percolation amount, I [mm] is the irrigation amount.

In this study, we defined a crop as being under drought exposure when the average water pressure head inside the root zone was below a specific pressure head threshold. The drought exposure ratio predictions are thus defined as the ratio of the cumulative number of times that a crop is under drought exposure over the total time-series data:

$$DE = \frac{1}{N}\sum\nolimits_{i=1}^{N} D_i, D_i = \begin{cases} 0 & h_t \le h_i \\ 1 & h_i < h_t \end{cases} \tag{2}$$

where DE [d d^{-1}] is the drought exposure ratio, i.e., the number of days with drought relative to the total number of days, h_t [cm] is the pressure head threshold below which drought stress is experienced, and h_i [cm] is the average pressure head in the root zone on day i. Here we used $h_t = -50$ cm on the EMMAN3G module (Mondaca-Duarte et al., 2020a, 2020b). The same computation was applied by (Mondaca-Duarte et al., 2020b), although then it was referred to as 'crop stress risk' instead of the drought exposure ratio, the latter being our preferred term for this study (Eq. 2).

2.4. Prediction uncertainty

The level of uncertainty in the evapotranspiration was calculated according to the methodology developed by (Mondaca-Duarte et al., 2020b). The model performance matrix was computed 100 times for each combination of frequency and irrigation dosage, using a Monte Carlo sampling method. The sampling was done at random, with each random daily evapotranspiration sample having the same probability of being selected. This yielded a discrete probability density function representing the uncertainty in evapotranspiration.

The evapotranspiration dataset included 32 measurement days, beginning on 31 July 2016. The evapotranspiration dataset was divided into 32 daily segments, which were used to artificially create variable evapotranspiration datasets by randomly drawing 32 segments and recreating a new 32-day dataset for each model computation. The schematic representation of how the uncertainty study was simulated is presented in Section 2.6.

The prediction uncertainty of leaching fraction and drought exposure was represented by the standard deviation as obtained from the 100 realizations. The uncertainty study was performed on 6 different types of greenhouse soils, divided into 3 sandy soils and 3 clay soils. The parameters for each soil type and each soil layer are presented in Table 1. These soil parameters are used by the van Genuchten-Mualem equation, where α [cm^{-1}], n and λ are shape parameters, θ_r [cm^3 cm^{-3}] is the residual water content, θ_s [cm^3 cm^{-3}] is the saturation water content, and K_s [cm d^{-1}] is the hydraulic conductivity at saturation. A detailed explanation of the equations used in this framework can be found in (Mondaca-Duarte et al., 2020b).

Contour plots were used to compare certain and uncertain leaching fractions, with their associated drought exposure predictions against each other. The plot for certain predictions uses a single evapotranspiration dataset. This means that there is no standard deviation. The visualization of uncertain predictions is done in a conservative way, where leaching and drought exposure are likely overestimated, as each point in the plot represents the average of the prediction plus two standard deviations. The two standard deviations were chosen to represent a worst case scenario where the contour plots would show the highest possible drought exposure and leaching fraction within 95% of the prediction distribution. A grower could consider this worst case

Table 1
Soil parameters from clay and sandy greenhouse soils, with their specific codes.

Soil type	Parameters					
Clay soils	α (cm^{-1})	n (-)	θ_r (cm^3 cm^{-3})	θ_s (cm^3 cm^{-3})	K_s (cm d^{-1})	λ (-)
Soil 1, Layer 1 (B9)	0.007	1.27	0.00	0.43	1.8	-2.38
Soil 1, Layer 2 (O10)	0.010	1.25	0.01	0.47	2.3	-0.79
Soil 1, Layer 3 (O10)	0.010	1.25	0.01	0.47	2.3	-0.79
Soil 2, Layer 1 (B7)	0.018	1.25	0.00	0.40	14.6	0.95
Soil 2, Layer 2 (O9)	0.010	1.38	0.00	0.46	3.8	-1.01
Soil 2, Layer 3 (O9)	0.010	1.38	0.00	0.46	3.8	-1.01
Soil 3, Layer 1 (B10)	0.013	1.14	0.01	0.45	3.8	4.58
Soil 3, Layer 2 (O10)	0.010	1.25	0.01	0.47	2.3	-0.79
Soil 3, Layer 3 (O9)	0.010	1.38	0.00	0.46	3.8	-1.01
Sandy Soils	$\boldsymbol{\alpha}$	$\boldsymbol{n}$	$\boldsymbol{\theta_r}$	$\boldsymbol{\theta_s}$	$\boldsymbol{K_s}$	$\boldsymbol{\lambda}$
Soil 1, Layer 1 (B2)	0.022	1.35	0.02	0.43	83.2	7.20
Soil 1, Layer 2 (O2)	0.016	1.52	0.02	0.39	22.8	2.44
Soil 1, Layer 3 (O2)	0.016	1.52	0.02	0.39	22.8	2.44
Soil 2, Layer 1 (B3)	0.015	1.51	0.02	0.44	19.1	0.14
Soil 2, Layer 2 (O3)	0.017	1.70	0.01	0.34	12.4	0.00
Soil 2, Layer 3 (O2)	0.016	1.52	0.02	0.39	22.8	2.44
Soil 3, Layer 1 (B3)	0.015	1.51	0.02	0.44	19.1	0.14
Soil 3, Layer 2 (B3)	0.015	1.51	0.02	0.44	19.1	0.14
Soil 3, Layer 3 (B3)	0.015	1.51	0.02	0.44	19.1	0.14

Source:Source: (Heinen et al. (2020).

scenario if he/she is risk averse, or could compare between certain and uncertain predictions and decide how much risk he/she is willing to take.

2.5. Smoothing noisy data

Leaching fraction and drought exposure outputs were noisy due to stochasticity in measured daily radiation. This noise was propagated into the isoline visualization of predictions. Given the high levels of the noise and its high level of dependency on the particular Monte Carlo sampling of the measurement data, and given that this noise obscures a clear view of the predicted leaching fraction and drought exposure isolines, the output was smoothed.

Data smoothing was performed using a moving-average smoothing algorithm in MATLAB 2021b, using the ‘smooth’ function on a data array. The array was smoothed using a 5-point moving average, meaning that it takes an average of 5 values to generate a single point, moving the average a single array value at a time and obtaining a new average single point. The smoothing was performed on both outputs (i.e. leaching fraction and drought exposure), starting with the row data array of the y-axis (dosage) and then proceeding to the column data array of the x-axis (frequency), from top to bottom and then from left to right.

2.6. Schematic representation

A ‘bird’s eye view’ of the model framework is presented in Fig. 2. Under the framework scheme, i and N from Eqs. 1 and 2 were renamed *i_data* and *data_end* for easier understanding of the model framework. The time-series length is *i_data* from 1 to *data_end*, where *data_end* is the total length of the time-series (N). The time-series includes solar radiation and air temperature. A matrix PRM_{f_dosage,f_freq} is made based on the evapotranspiration demand calculated according to the de Graaf model. This matrix indicates the irrigation (*irr*) of a specific frequency (*f_freq*) and dosage (*f_dosage*) described in Section 2.2.

The framework uses a two-nested for-loop to examine each entry on the performance matrix, based on the frequency and dosage. Each entry uses the complete time-series data to give predictions on the drought exposure ratio and leaching fraction for that specific dosage and frequency. The first loop ends once dosage (*f_dosage*) reaches the final range value (*dosage_end*), the next frequency (*f_freq*) value is chosen, and the dosage is reset to the first dosage value. The second loop continues until the frequency (*f_freq*) reaches the final range value (*freq_end*).

Inputs for the EMMAN3G model include the irrigation value, evapotranspiration, soil parameters for three different soil layers and air temperature. A specific soil type is selected along with its soil parameters. The EMMAN3G model outputs are the soil water pressure head and soil percolation values. If the evapotranspiration is selected to be uncertain, the simulations are iterated a certain number of iterations (each iteration is denoted with index *iter_run* with $iter\_run = 1..iter\_total$. In this study, $iter\_total = 100$. Cumulative soil percolation (Sp_{iter_run}), soil pressure head (h_{iter_run}) and crop drought exposure are stored. When the total *iter_run* iterations are computed, the mean and standard deviation of the soil percolation and pressure head are stored for use in the performance matrix plot as the leaching fraction ratio and the drought exposure ratio.

2.7. Comparison between clay and sandy soil

The mean of the mean for each of the three sandy soil types, and the mean of the mean for each of the three clay soils types was used to compare the differences in drought exposure and leaching fraction between clay and sandy soils. The mean of the mean values were sorted using MATLAB *cat*() function. The mean of the mean is from now on referred to as the overall mean. The standard deviation of the overall mean was also obtained.

The arrays were visualized using MATLAB’s contour plot *contourf*, creating a filled contour plot with isolines. Contour plots of the overall mean were created, as well as a contour showing the difference of the mean values between clay and sandy soils. Finally, contour plots for the overall mean standard deviation were also created.

3. Results and discussion

3.1. Smoothing plot

Fig. 3 illustrates how smoothing using moving averages clarifies the distinction between the different levels of drought exposure ratio. This is important when selecting an irrigation strategy, especially for strategies calling for fewer days between irrigation and with lower leaching fractions. If there is not a clear distinction between the regions of drought exposure ratio or leaching fraction, it becomes harder to select an irrigation strategy, especially for lower frequency predictions (as displayed in Fig. 3).

3.2. Model-based irrigation analysis

Each element of the array of the framework matrix contains the value of drought exposure, leaching fraction, and their respective standard deviation, if uncertainty is included, for a specific dosage of total irrigation and frequency of irrigation. This amount of data makes it hard to

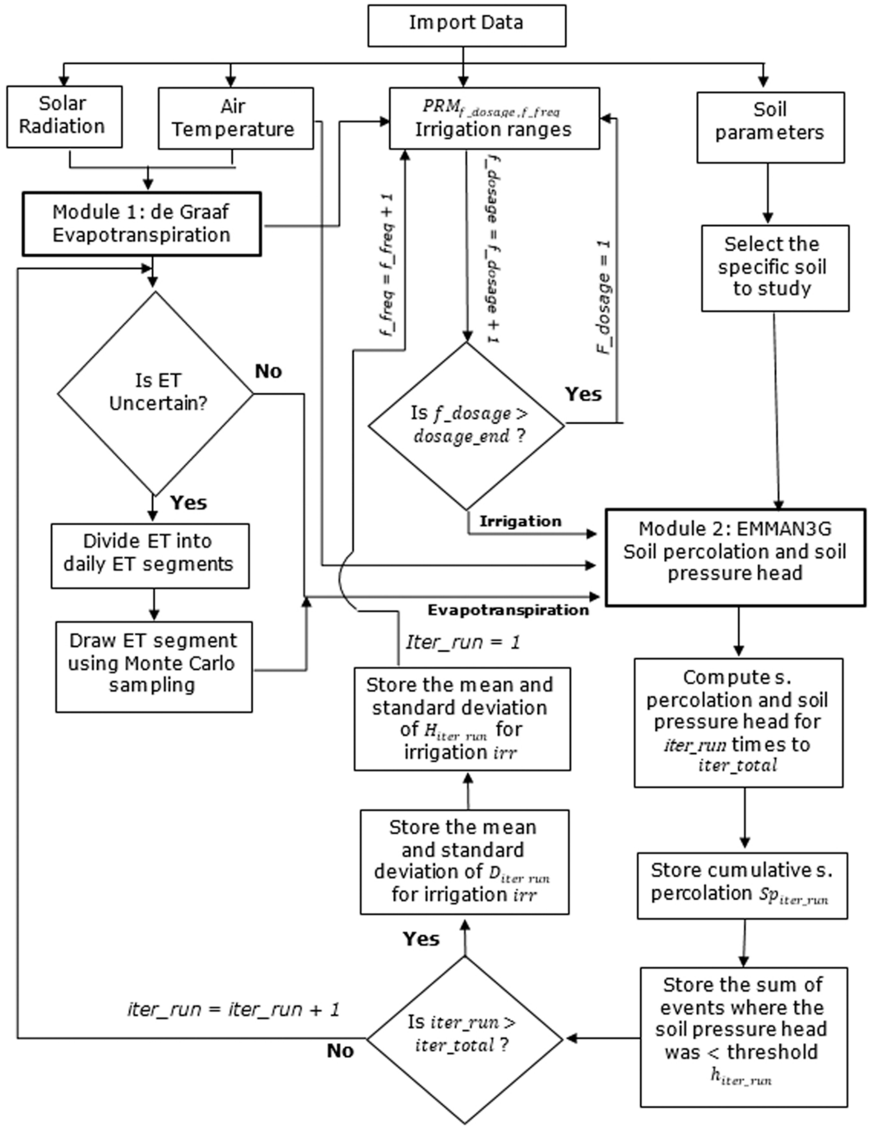

Fig. 2. Schematic representation of the model-based framework modified from the framework in (Mondaca-Duarte et al., 2020b).

visualize the standard deviation individually. For this reason, this section includes three specific total irrigation dosages where drought exposure and leaching fraction predictions, along with their plus one and plus two standard deviations, can be observed (Figs. 4 and 5). A visualization of certain predictions for all the total irrigation values is shown in Section 3.3, and a visualization of uncertain predictions for all the total irrigation values is shown in Section 3.4.

Fig. 4 shows the drought exposure at 114 mm, 140 mm, and 154 mm of total irrigation. Fig. 5 shows the leaching fraction at the same irrigation values. These specific irrigation values represent: 1) the calculated total evapotranspiration (114 mm), 2) an irrigation mid-point with sufficient leaching fraction (140 mm), and 3) the total irrigation from experiment values (154 mm).

The drought exposure increases as the irrigation frequency decreases, even for high irrigation dosages of up to 150% evapotranspiration (154 mm). The confidence intervals become larger as the days between irrigation increase. For one or more irrigations per day, the drought exposure becomes negligible. With an irrigation near evapotranspiration (114 mm) the drought exposure starts to increase after frequencies higher than once per day. Additionally, the confidence interval that represents uncertainty of drought exposure increases when the irrigation rate approaches the evapotranspiration rate.

Fig. 4 shows that an irrigation strategy where total water gift approaches total evapotranspiration (top plot) will require a higher irrigation frequency to maintain a low drought exposure ratio. For growers, this means that reducing the total irrigation would require an increase in irrigation frequency to prevent exposing their crop to higher ratios of drought exposure.

As such, the precision of irrigation management becomes even more critical, emphasizing the importance of applying irrigation on an hourly basis, when the technical systems allows it. Hourly irrigation ensures that crops receive precise amounts of water, avoiding under- or overwatering, leading to improved crop yields, reduce water use and have less uncertainty in drought exposure.

Fig. 5 shows that the leaching fraction increases the higher the total irrigation and the higher the days between irrigation. On the other hand, compared to the drought exposure, the leaching fraction confidence interval is nearly independent of the number of days between irrigation, as well as of the total irrigation values.

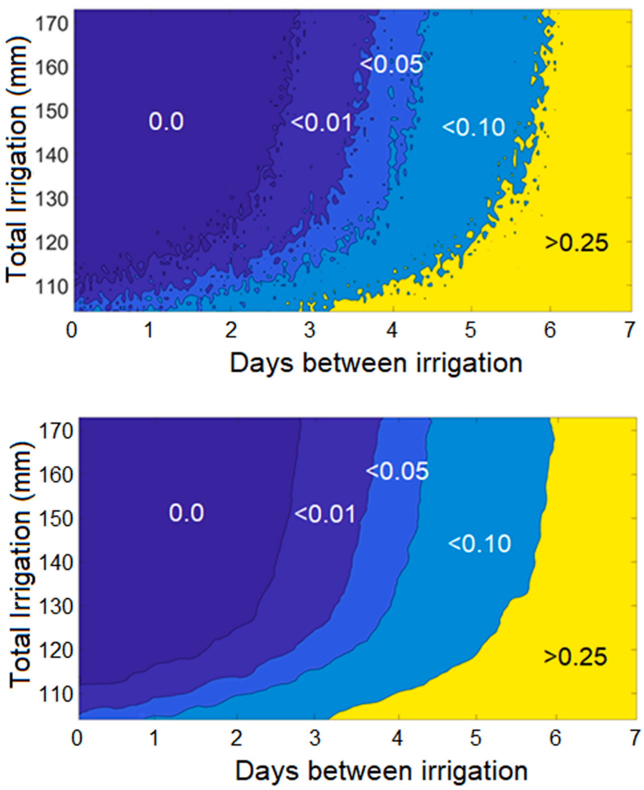

Fig. 3. Top: Prediction of drought exposure in a clay soil (Clay soil 1, Table 1). The x-axis represents the days between irrigation (frequency), and the y-axis represents the total irrigation (dosage). The drought exposure ratio changes depending on the isoline region, with the far left area representing zero drought exposure, followed by drought exposure ratio values of < 0.01, < 0.05, < 0.10, and with the far right region having values of > 0.25 for the drought exposure ratio. Bottom: drought exposure ratio prediction after application of the moving average smoothing method on the upper graph.

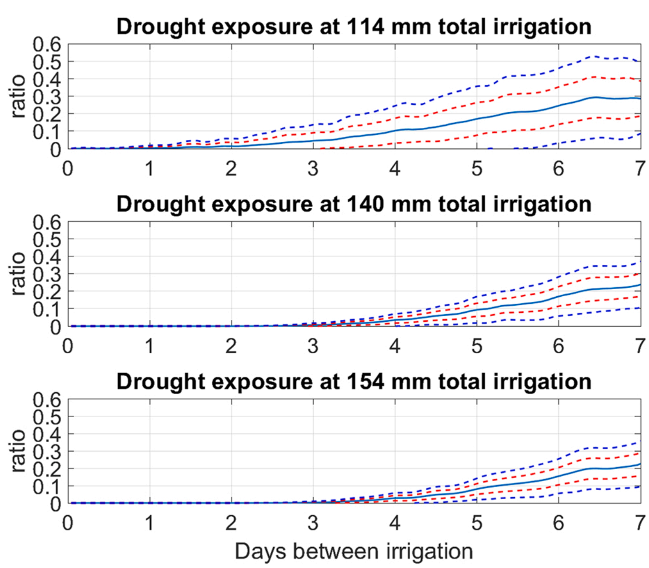

Fig. 4. Prediction of drought exposure (DE) in a clay soil (clay soils 3, Table 1), with uncertain evapotranspiration at three different total irrigation values. Top: 114 mm, Middle: 140 mm, Bottom: 154 mm. The red inner dashed lines represent the mean plus and minus 1 standard deviation. The blue outer dashed lines represent the mean plus and minus 2 standard deviations.

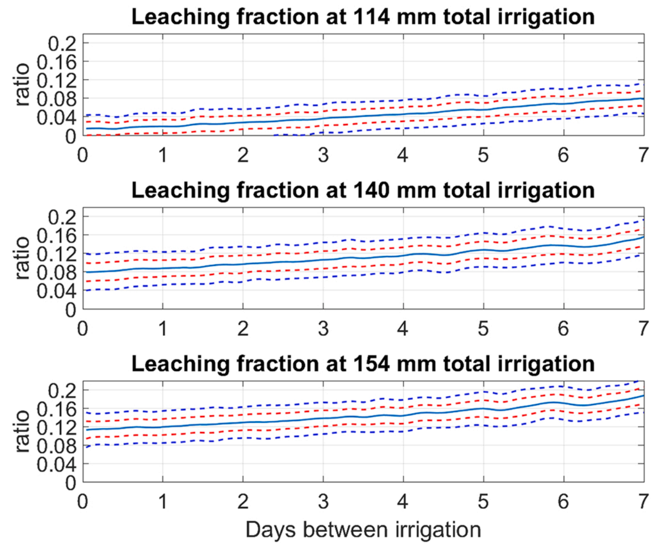

Fig. 5. Prediction of leaching fraction in a clay soil (clay soils 3, Table 1), with uncertain evapotranspiration at three different total irrigation values. Top: 114 mm, Middle: 140 mm, Bottom: 154 mm. The red inner dashed lines represent the mean plus and minus 1 standard deviation. The blue outer dashed lines represent the mean plus and minus 2 standard deviations.

3.3. Prediction with certain evapotranspiration

Drought exposure and leaching fraction predictions are shown in Fig. 6. An ideal irrigation strategy minimizes water use and drought exposure, while simultaneously maintaining a desired leaching fraction. This means that, for example, for a particular soil type with a desired LF of 10% (or LF $= 0.1$ as in Fig. 6), an irrigation strategy of 140 mm with an irrigation frequency of once every two days would have a predicted DE of < 0.01.

These results are comparable to the results in (Turan et al., 2015), when scaled back to a 32-day period as in our study. In that work it was found that an interval of 2 or 4 days irrigation with an irrigation amount of 131.4 mm can be used to save water without affecting crop quality. This is in line with our predictions. Fig. 4 indicates that if the days between irrigation are 2 or 3, there will be no drought exposure.

Comparing the model-based predictions with the lysimeter experimental data (indicated by the dot and arrow in Fig. 6) reveals that, when no uncertainty in evapotranspiration is considered, the irrigation strategy during the greenhouse experiment involving an irrigation frequency of once every three days and total irrigation of 154 mm was a safe choice, with DE levels below 0.01 and a LF of 0.15.

These model predictions can be used to give irrigation advice. Growers could adjust both, dosage and frequency of irrigation, to obtain significant reductions in water use. For example, a grower could use a dosage of 140 mm and a frequency of once every two days to reduce soil percolation by 40% and water use by 9%, relative to the experimental irrigation strategy (dosage of 154 mm and frequency of once every three days), while maintaining a leaching fraction above 10%.

Given a predefined drought exposure ratio, results indicate that different combinations of frequency and dosage of irrigation lead to the same level of drought exposure, as well as different combinations of inputs producing a similar leaching fraction. This observation suggests that selecting the appropriate frequency and dosage of irrigation is a multi-objective optimization problem. As Fig. 6 demonstrates, given a required maximum drought exposure ratio, a different combination of dosage and frequency of irrigation can have the same leaching fraction. Similarly, given a required maximum leaching, different combinations of dosage and frequency will yield the same values of drought exposure risk.

If low drought exposure is desired, Fig. 6 indicates that frequencies

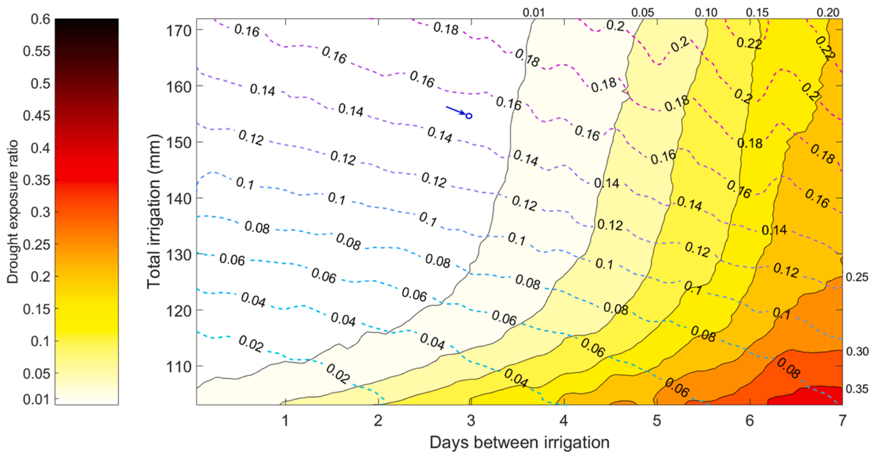

Fig. 6. Prediction of drought exposure (DE) and leaching fraction (LF) in a clay soil (Clay soil 3, Table 1), with certain evapotranspiration. The arrow and symbol is the LF, and DE ratio obtained from the cumulative soil percolation from the lysimeter measurements, based on experimental data. The frequency of irrigation in days is charted along the x-axis, with the y-axis representing the total irrigation dosage. The solid isolines indicate the ratio of days under the drought exposure threshold (left bar), and the dashed isolines represent the leaching fraction predictions. The isoline values are given at the outer edge of the plot.

lower than once per 3.5 days will not be feasible in practice. For example, if a grower wants a total drought exposure of < 0.01, then the number days between irrigation must be lower than 3.5; a higher number will result in extremely high required dosages, which is a result of the almost vertical isolines for periods larger than 3.5 days combined with total irrigation higher than 130 mm.

For any specific combination between drought exposure ratio and leaching fraction, only a single combination of irrigation dosage and frequency will be able to achieve it. This is due to the fact that the drought exposure and leaching fraction isolines are more or less perpendicular to each other. However, if the requirement is to achieve a leaching fraction and drought exposure within some range, multiple combinations of dosage and frequency will be able to achieve it. This can be useful to a grower as a single combination or the array of allowed combinations are relatively easily recognized in Fig. 6.

The performance matrix thus offers a good way of identifying a suitable strategy for a specific requirement, allowing growers the freedom to choose a combination of frequency and dosage that suits their needs. These needs depend on available equipment and on performance requirements. For example, for certain fruit crops it is known that a slight drought (or salinity) stress results in improved fruit quality (Wang et al., 2019).

3.4. Prediction with uncertain evapotranspiration

Drought exposure and leaching fraction predictions in Fig. 7 are shown as the mean plus two standard deviations (representing a worst case scenario of uncertain evapotranspiration). When evapotranspiration becomes uncertain, the predicted DE increases, shifting the isolines towards higher frequencies and dosages of irrigation (as compared to Fig. 6).

When certain and uncertain predictions are compared, it is shown that combinations of frequency and dosage give different leaching fraction (LF) values. For example, certain predictions in Fig. 6 at an irrigation of 150 mm with 3 days between irrigation show a LF of 0.14. Uncertain predictions in Fig. 7 show a LF of 0.16 at the same frequency and dosage. Regarding drought exposure (DE), uncertain predictions have fewer possible combinations of dosage and frequency with DE values below 0.01.

Comparing the model-based predictions with the lysimeter experimental data (indicated by the symbol and arrow in Fig. 7) reveals that the irrigation strategy based on experimental data now have a drought exposure of 0.1. So, the grower would require to adjust the dosage and/or frequency to reduce the drought exposure ratio.

Being able to give advice under uncertainty is decisive because, with these model predictions, growers can avoid drought exposure even when the evapotranspiration is not certain. A grower must select either a more conservative strategy, thereby increasing both water use and leaching fraction, or a strategy that will increase the ratio of drought exposure. Given that growers are generally risk-averse, they are likely to select more conservative strategies.

Additionally, economic farm requirements like labour or equipment also play a role in selecting an irrigation strategy. Therefore, it is quite important to consider the uncertainty in the model predictions, so growers can receive accurate advice that does not impact negatively these economic requirements. For example, Chrysanthemum growers require a dryer soil surface for certain periods where labour and equipment are used for agricultural practices such as spraying plant

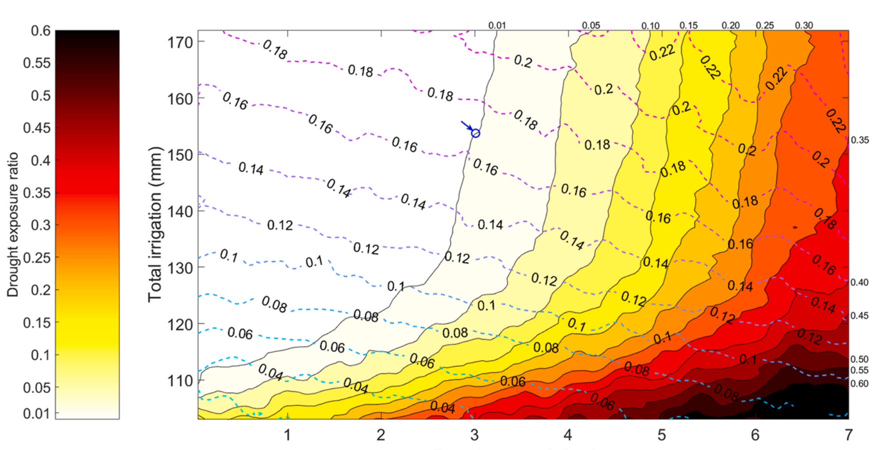

Fig. 7. Prediction of drought exposure and leaching fraction (LF) in a clay soil (Clay soil 3, Table 1), with uncertain evapotranspiration. The arrow and symbol is the LF, and DE ratio obtained from the cumulative soil percolation from the lysimeter measurements, based on experimental data. The frequency of irrigation in days is charted along the x-axis, with the y-axis representing the total irrigation dosage. The solid isolines indicate the ratio of days under the drought exposure threshold (left bar), and the dashed isolines represent the leaching fraction predictions. The solid isoline values are given at the outer edge of the plot.

protective products, removal of old leaves, or flower harvest. If an uncertain strategy is selected, with too few days between irrigation, the soil surface will remain wet and the growers will have a hard time performing these agricultural practices.

3.5. Comparison between clay and sandy soil types

3.5.1. Leaching fraction variation

The overall mean values of leaching fraction from the three different sandy soil types explored in this study are represented in Fig. 8. The overall mean leaching fraction values for the clay soils are presented in Fig. 9. The difference between the overall mean values of sandy soils minus clay soils are presented in Fig. 10.

Sandy soils have a slightly higher leaching fraction than clay soils (Fig. 10). The higher total irrigation and longer days between irrigations increase the difference in leaching fraction. This increase in leaching fraction difference does play a role when choosing a combination of dosage and frequency for an irrigation strategy but only when high dosages and longer days between irrigation are considered, which usually is not the case.

Irrigation strategies normally aim to have a low leaching fraction. For example, if a grower considers to have a standard leaching fraction value of 0.1, the highest total irrigation would be on sandy soils at 145 mm on frequencies below one day between irrigation (Fig. 8). At that dosage and frequency, the highest leaching fraction difference would be 0.008, which is only an 8% variation compared to the leaching fraction of 0.1. This means that the model predictions can be used to give certain irrigation advice regarding leaching fraction for commonly used strategies across different types of soil.

3.5.2. Drought exposure variation

The overall mean drought exposure values from the three different sandy soil types explored in this study are represented in Fig. 11. The overall mean drought exposure values for the clay soils are presented in Fig. 12. The difference between the overall mean values of sandy soils minus clay soils are presented in Fig. 13.

A clear relation between the type of soil and drought exposure can be seen. Overall, sandy soils tend to have a higher drought exposure than clay soils. This is expected, as sandy soils have a higher hydraulic conductivity and lower water holding capacity (water availability; see, e.g., (Heinen et al., 2021), increasing the possibility of drought. On average, the studied sandy soils require irrigation frequencies of more than once per 3 days (Fig. 11).

There is an interesting response on certain combinations of irrigation frequencies and total irrigation (Fig. 13). Looking at different dosage and frequency values two things can be observed.

First, when an irrigation strategy has a high total irrigation (above 155 mm), the difference in drought exposure between sandy and clay soils becomes close to zero. This is because at frequencies less than once per 3 days, the water status at the first soil layer never goes below the threshold in both types of soil, so the difference is zero as both soils have zero drought exposure.

Second, when the total irrigation is below 125 mm and the days between irrigation are above 1 day, then the sandy soils present higher drought exposure compared to clay soils. For example, in Fig. 13, DE difference of 0.1 is present at a total irrigation of 120 mm and days between irrigation below 1 day, and it follows a contour along a change in frequency and dosage up to 150 mm at a frequency of 5 days between irrigation. This can be explained because for fully grown crops the evapotranspiration rate is approximately the same for both soils, but the water flow rate to the second layer is higher in sandy soils, increasing the drought exposure compared to clay soils.

It is interesting that there are combinations of dosage and frequency where the drought exposure difference is zero across multiple types of soil. Using the model framework predictions for irrigation advice, growers can consider these combinations of dosages and frequencies regardless of the type of soil they have. However, some of these combinations require higher total irrigation dosages, which increases soil percolation, and in some cases it is not desired.

3.6. Standard deviation of the mean between soil types

3.6.1. Leaching fraction

The standard deviation of leaching fraction in clay soils (Fig. 14) and sandy soils (Fig. 15) are shown in this section. There is a considerable difference in standard deviation between sandy soils and clay soils. The standard deviations in clay soils range from 0.02 to 0.03 for almost all combinations of dosage and frequency. Fig. 15 shows that sandy soils have a high uniformity in standard deviation (0.005–0.01) compared to clay soils.

An explanation of this difference in standard deviation between soils is that water retention is especially sensitive to the variation in composition of clay soils. In clay soils, water is held more tightly and moves more slowly through the soil compared to sandy soils. The small pores in clay soils allow water to be held tightly, whereas the large pores in sandy soils allow water to move through the soil at a higher rate. This is quite important, as it shows the model is quite certain in leaching fraction predictions, especially on sandy soils.

The highest standard deviation was 0.03, on clay soils. This represents a high variation as the mean leaching fraction values at that dosage

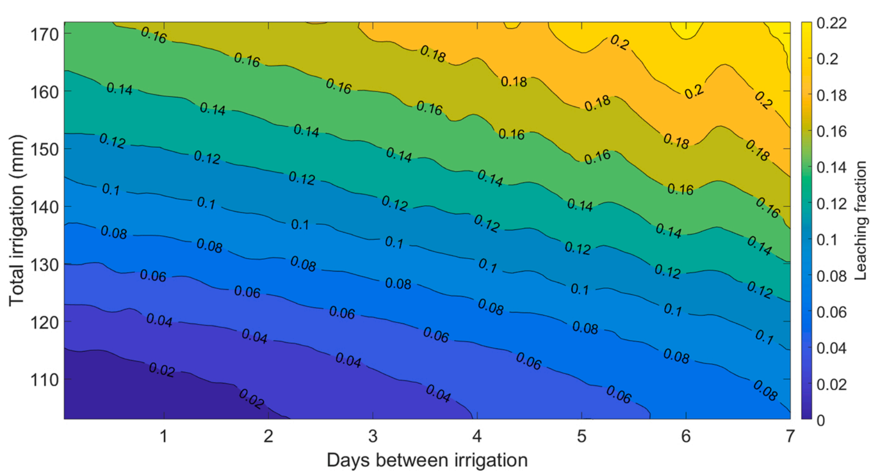

Fig. 8. Contour plot of the leaching fraction overall mean values taken over sandy soils 1, 2, and 3, with different irrigation frequencies on the x-axis, and total irrigation dosages on the y-axis.

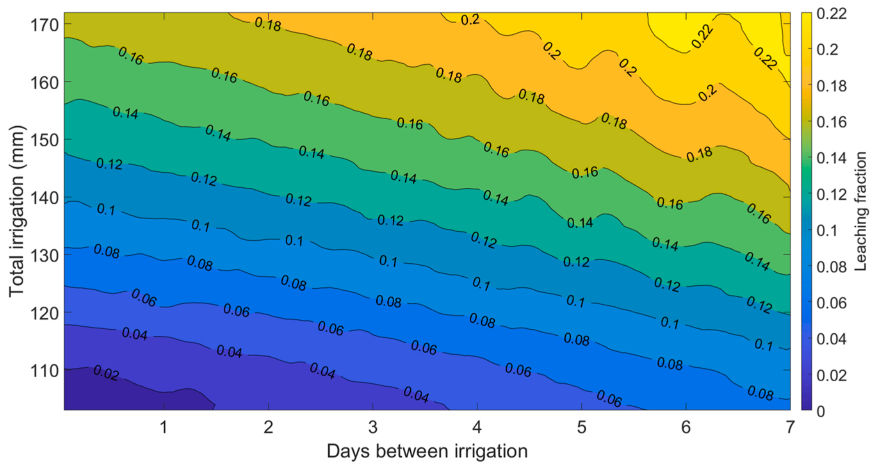

Fig. 9. Contour plot of the leaching fraction overall mean values taken over clay soils 1, 2, and 3, with different irrigation frequencies on the x-axis, and total irrigation dosages on the y-axis.

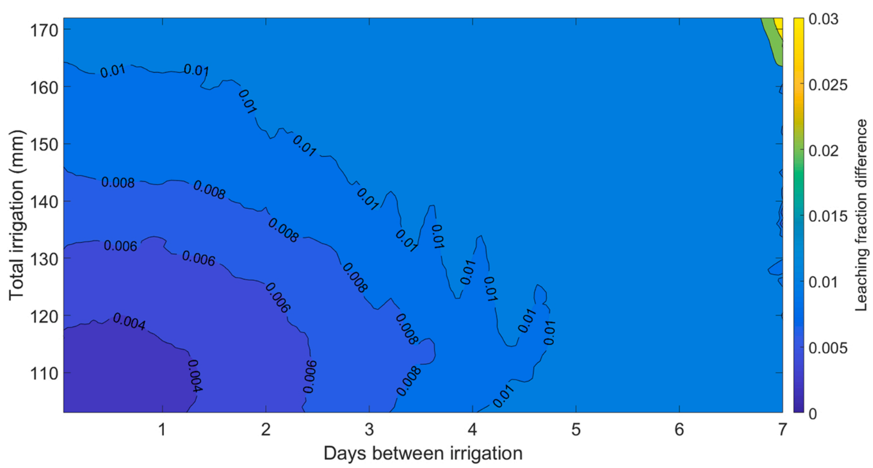

Fig. 10. Contour plot of the difference in leaching fraction overall mean values between sandy soils minus clay soils, with different irrigation frequencies on the x-axis, and total irrigation dosages on the y-axis.

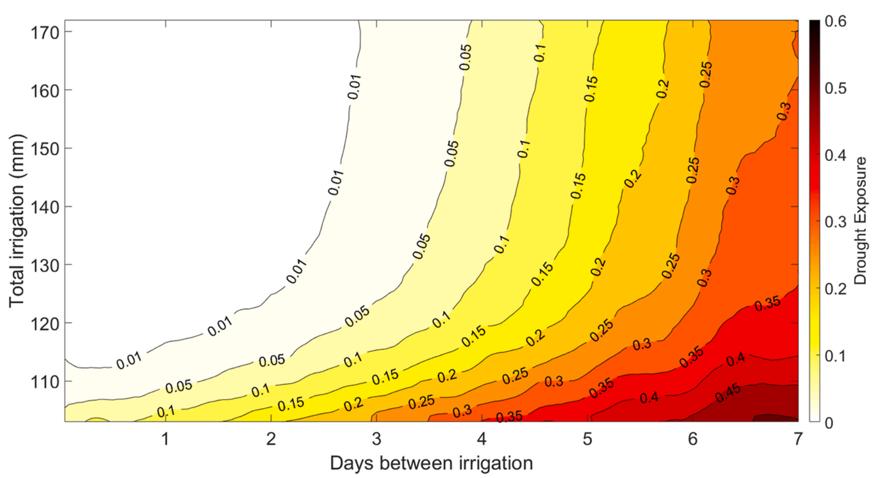

Fig. 11. Contour plot of the drought exposure overall mean values taken over sandy soils 1, 2, and 3, with different irrigation frequencies on the x-axis, and total irrigation dosages on the y-axis.

and frequency was 0.06. This means that predictions from the model will be uncertain when giving irrigation advice on clay soils. When using the model framework predictions to give irrigation advice to growers with clay soils, growers need to be certain about the specific soil parameters of their soil to reduce the deviation between clay soils.

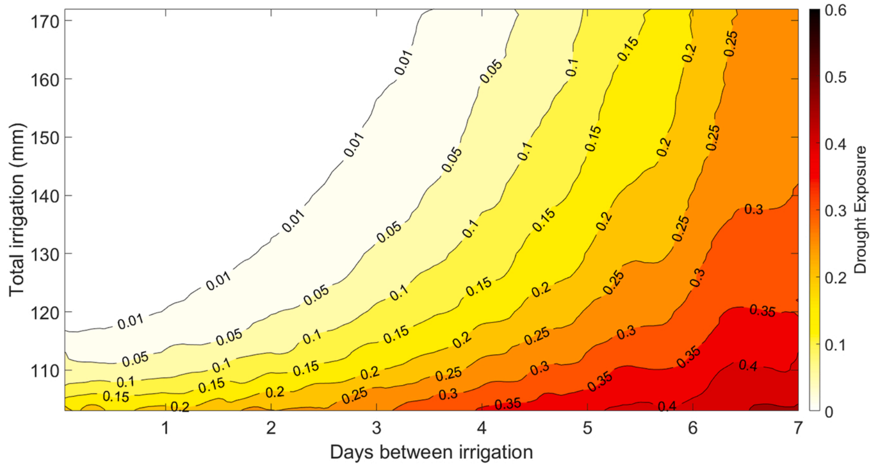

Fig. 12. Contour plot of the drought exposure overall mean values taken over clay soils 1, 2, and 3, with different irrigation frequencies on the x-axis, and total irrigation dosages on the y-axis.

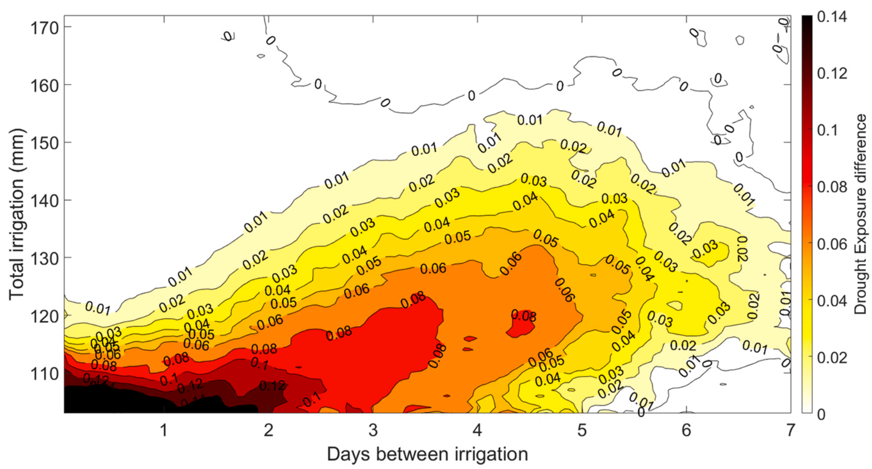

Fig. 13. Contour plot of the difference in drought exposure overall mean values between clay soils and sandy soils, with different irrigation frequencies on the x-axis, and total irrigation dosages on the y-axis.

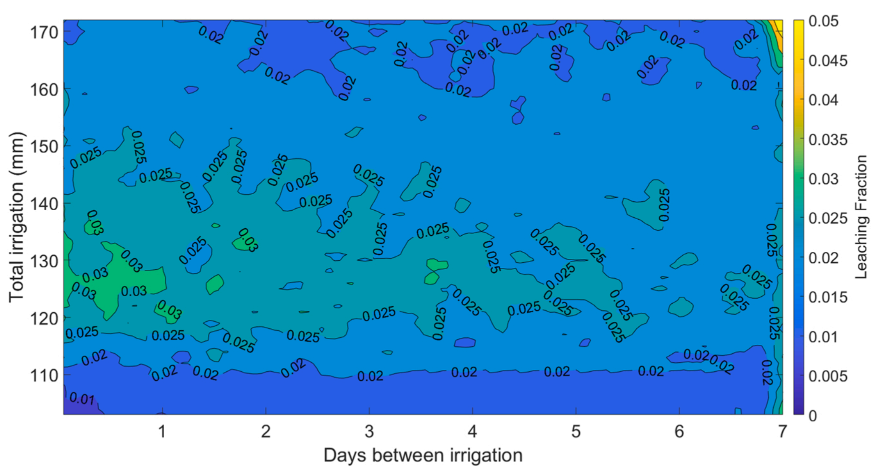

Fig. 14. Contour plot of the leaching fraction standard deviation of the mean values over clay soils 1, 2, and 3, with different irrigation frequencies on the x-axis, and total irrigation dosages on the y-axis.

3.6.2. *Drought exposure*

The standard deviation of drought exposure in clay soils (Fig. 16) and sandy soils (Fig. 17) are shown in this section. Considering the standard deviation between the same types of soil can provide insight in how certain or uncertain can the model predictions be with similar types of soil.

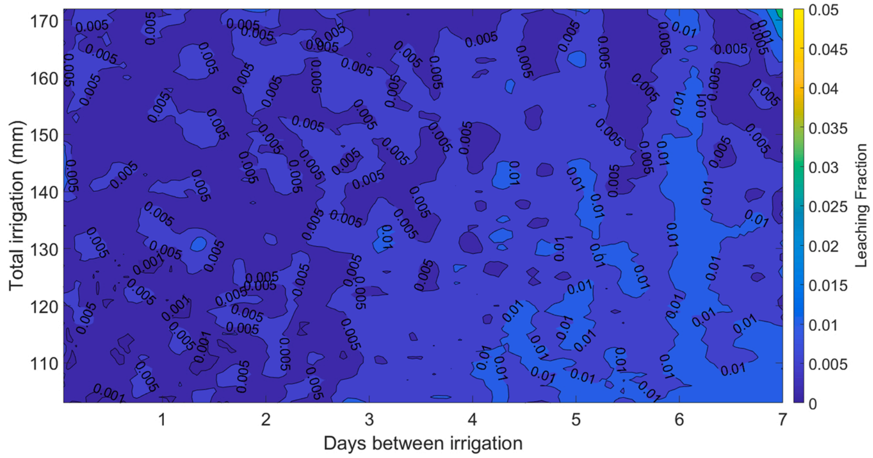

Fig. 15. Contour plot of the leaching fraction standard deviation of the mean values over sandy soils 1, 2, and 3, with different irrigation frequencies on the x-axis, and total irrigation dosages on the y-axis.

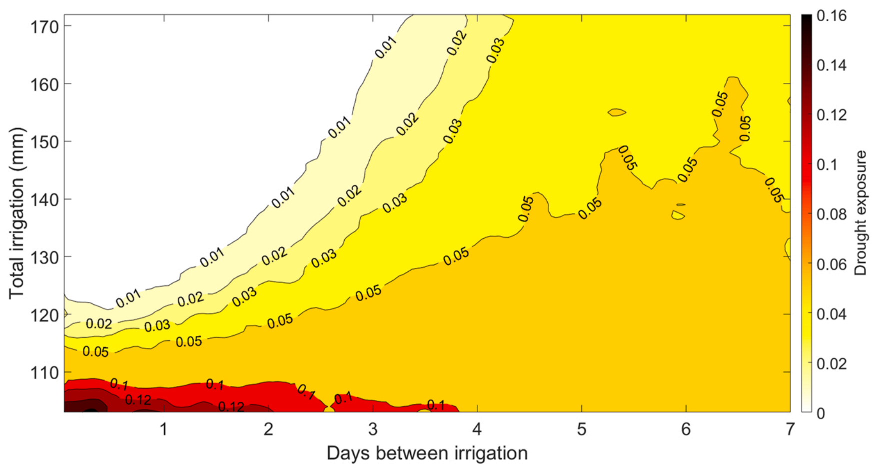

Fig. 16. Contour plot of the drought exposure standard deviation values over clay soils 1, 2, and 3, with different irrigation frequencies on the x-axis, and total irrigation dosages on the y-axis.

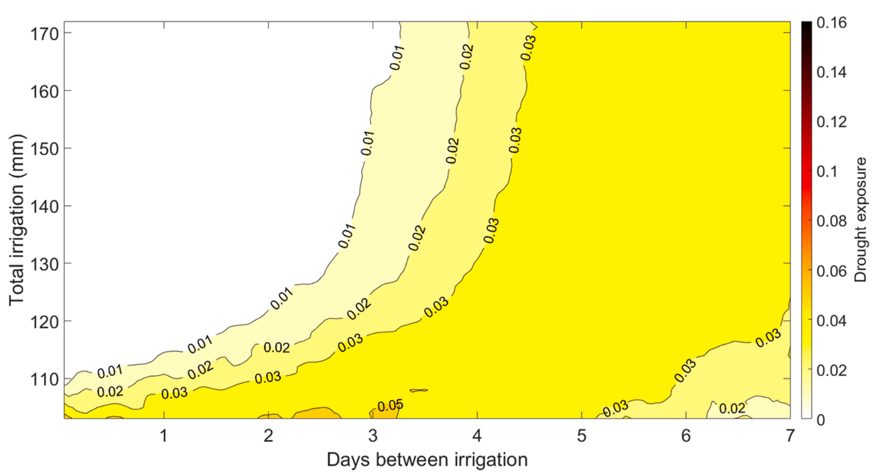

Fig. 17. Contour plot of the drought exposure standard deviation values of sandy soils 1, 2, and 3, with different irrigation frequencies on the x-axis, and total irrigation dosages on the y-axis.

Figs. 16 and 17 show that there are combinations of dosage and frequency where the predicted drought exposure has a standard deviation below 0.01, making predictions with these combinations highly certain. These certain predictions can be traced at frequencies of less than one day between irrigation, and total irrigation dosages on clay soils starting above 125 mm, and sandy soils starting above 112 mm. To maintain these certain predictions at higher days between irrigation, it is required to increase the total irrigation.

A comparison between both soils shows that sandy soils require less total irrigation to maintain the drought exposure deviation below 0.01 up to a sudden increase in required total irrigation at days between irrigation above 3 days. Another observation is that overall, clay soils present less certain predictions compared to sandy soils, where values of standard deviation above 0.05 are present in several dosage and frequency combinations compare to almost none in sandy soils.

This difference in the standard deviation of drought exposure between clay and sandy soils can be explained similarly as the leaching fraction deviation. There is more variation in water retention in clay soils than sandy soils, as clay soils water retention can vary from different clay soil sources.

Standard deviation of drought exposure can give insight in how certain an irrigation strategy advice can be across a type of soil. If growers know they have a crop on a type of soil, but are not certain about its specific soil parameters, they can use the model framework to plan an irrigation strategy that can avoid this uncertainty. Also, in cases where they have clay soil, growers would require to be aware that there is higher deviation in predictions when using some combinations of dosages and frequencies.

3.7. Limitations and improvements in the model framework

The model framework considers drought exposure as the ratio between the amount of hours a crop is under a specific pressure head threshold compared to the total amount of hours. However, this ratio does not consider if those hours were consecutive or along a specific timeline. This means that you can have the same drought exposure prediction if a crop was 48 consecutive hours below the threshold during a 48 day period, or if a crop is one hour each day for a 48 day period below the threshold.

Right now we use a simple metric of ratio of hours above a certain threshold, but it could be explored as a pattern of drought periods with different intensities in pressure head, as well as cumulative number of hours between these drought periods, giving a more detailed advice regarding if a crop is stressed or not.

The model framework uses global radiation to predict evapotranspiration. At the same time, uncertainty in evapotranspiration is considered as a variation in daily global radiation. However, once a frequency and dosage is put into the model, the irrigation amount does not change, even if the global radiation is high between irrigation events. This means that between those irrigation events the irrigation might not have been enough.

It would be interesting to address changes in between irrigation events and see how the model predictions respond to them. If we can change the dosing in between irrigation based on variables like cumulative radiation, temperature or crop growth then the model can respond in a more dynamic way. Therefore, it could be worthwhile to extend the framework presented here with a method that considers feedback from these variables and adjust the dosage or frequency.

The experimental data used to verify the model considers a full grown Chrysanthemum crop in a 32 day period. It would be interesting to use the model framework to estimate the water requirements for a full growing period with the right data and by considering the development stages of the crop. One way to accomplish this is by incorporating the crop height as a variable in the model. As the crop grows, its water requirements change, and by adjusting the model parameters accordingly, it is possible to obtain estimates of the water needs for the whole growing period.

For this reason, it is advisable to extend this model-based approach using data from a whole cropping season, and even for multiple cropping seasons using multiple weather data from different regions, and multiple crops. The De Graaf model has a library of different crop factors for different types of crop which can be of interest to verify them with experimental data, and it can be even further extended to include models other than De Graaf, that also provide ET calculations.

Another limitation of our model framework is the potential impact of autocorrelation on the generated random evapotranspiration series. While we acknowledge that our sampling strategy using one day segments preserved the autocorrelation within a day, there may still be some autocorrelation for periods longer than a day that we did not account for in our analysis. This might potentially lead to differences between our simulated evapotranspiration data and the actual evapotranspiration values.

To address this issue, future studies could explore alternative sampling strategies or statistical methods that explicitly account for autocorrelation in the data. For instance, use block resampling techniques to generate multiple random samples of evapotranspiration data that account for the autocorrelation structure of the original data, that will help us to better understand the underlying autocorrelation structure of the ET data. In addition, collecting longer-term data series with higher temporal resolution can provide us with a more detailed information on how evapotranspiration varies throughout the day, and could help to better understand the autocorrelation patterns in the data.

The model framework assumes a fixed groundwater level as the bottom boundary condition. In modelling greenhouse cropping systems is a commonly used approach to simulate conditions that are typically found in areas where groundwater is managed through a drainage system, like in the Netherlands. However, this assumption may not always be valid in all situations, and its limitations must be acknowledged to ensure that the results of the study are not misinterpreted.

To address this limitation, a possible approach is to incorporate a variable groundwater level in the framework model. This would involve using data on groundwater levels from the specific region where the model is being applied, and incorporating this data into the model. The model would then simulate the actual conditions in the region, including fluctuations in groundwater levels, which would provide more accurate results. Additionally, as the groundwater is variable, it would be interesting to include an uncertainty analysis on the effect this variation on the water interactions between the soil layers, and consequently on the model results.

The model framework considers irrigation to be uniform per square meter area. In reality, irrigation is seldomly uniform and this can lead to cases where uneven irrigation can cause drought exposure. A new interesting approach could be to include sources of water giving at specific point of a studied area, and investigate to what extent these spatial variations in irrigation may improve performance predictions of drought exposure, leaching, and water use efficiency. A possible methodology to apply this approach would require to expand the 1D EMMAN3G model to a 2D soil water model, that considers water flow not just vertically but also horizontally.

4. Conclusions

The findings of this study provide valuable insights in irrigation strategies. The results demonstrate that modifying the dosage and frequency of irrigation can significantly reduce water use and leaching. This study also highlights the significant impact of evapotranspiration uncertainty on drought exposure and leaching predictions, emphasizing the need for low-risk irrigation strategies that consider this uncertainty.

Furthermore, this study shows that the shapes of the isolines, for both types of soil, indicates a high sensitivity of drought exposure ratio towards irrigation frequency, particularly for high total dosages. This finding suggests that careful consideration of irrigation frequency is crucial to ensure an optimal irrigation and reduce drought exposure. This study also points out the impact of soil type on predicted drought exposure and leaching, with clay soils showing more variation in these predictions compared to sandy soils.

Finally, a visualization of the predictions allows to identify possible combinations of irrigation dosage and leaching fractions, and supports growers into being informed about the effects and risks associated with their management decisions. This approach is fundamentally different from conventional optimization, which involves the computation of a single input strategy: the one that optimizes a selected performance criterion.

Declaration of Competing Interest

The authors declare the following financial interests/personal relationships which may be considered as potential competing interests Francisco D. Mondaca Duarte reports financial support was provided by National Council on Science and Technology.

Data Availability

Data will be made available on request.

Acknowledgements

We would like to thank the Consejo Nacional de Ciencias y Tecnologia (CoNaCyT) for their financial support for the first author under CVU: 446922. We are also grateful to Letsgrow.com for providing the lysimeter and climate data used in this work.

Appendix A. Supporting information

Supplementary data associated with this article can be found in the online version at doi:10.1016/j.agwat.2023.108301.

References

Abd El-Mageed, T.A., Semida, W.M., Taha, R.S., Rady, M.M., 2018. Effect of summer-fall deficit irrigation on morpho-physiological, anatomical responses, fruit yield and water use efficiency of cucumber under salt affected soil. Sci. Hortic. 237, 148–155. https://doi.org/10.1016/J.SCIENTA.2018.04.014.

Aggarwal, P.K., 1995. Uncertainties in crop, soil and weather inputs used in growth models: Implications for simulated outputs and their applications. Agric. Syst. 48, 361–384. https://doi.org/10.1016/0308-521X(94)00018-M.

Ayers, R.S., Westcot, D.W., Nations, F. and A.O. of the U, 1985. Water quality for agriculture LK - ⟨https://wur.on.worldcat.org/oclc/13182908⟩, FAO irrigation and drainage paper; 29, rev. 1 TA - TT -. Food and Agriculture Organization of the United Nations, Rome SE - xii, 174 pages: illustrations; 30 cm.

Delgoda, D., Malano, H., Saleem, S.K., Halgamuge, M.N., 2017. A novel generic optimization method for irrigation scheduling under multiple objectives and multiple hierarchical layers in a canal network. Adv. Water Resour. 105, 188–204. https://doi.org/10.1016/j.advwatres.2017.04.025.

Erisman, J.W., Galloway, J., Seitzinger, S., Bleeker, A., Butterbach-Bahl, K., 2011. Reactive nitrogen in the environment and its effect on climate change. Curr. Opin. Environ. Sustain. 3, 281–290. https://doi.org/10.1016/J.COSUST.2011.08.012.

Ertek, A., Şensoy, S., Küçükyumuk, C., Gedik, İ., 2004. Irrigation frequency and amount affect yield components of summer squash (Cucurbita pepo L.). Agric. Water Manag. 67, 63–76. https://doi.org/10.1016/J.AGWAT.2003.12.004.

FAO, 2016. AQUASTAT Main Database. Food and Agriculture Organization of the United Nations [WWW Document]. URL ⟨http://www.fao.org/nr/water/aquastat/main/index.stm⟩.

Heinen, M., 2001. FUSSIM2: brief description of the simulation model and application to fertigation scenarios. Agronomie 21, 285–296.

Heinen, M., Bakker, G., Wösten, J.H.M., 2020. Waterretentie- en doorlatendheidskarakteristieken van boven- en ondergronden in Nederland: de Staringreeks. Update 2018, Wageningen Environmental Research rapport BT - Waterretentie- en doorlatendheidskarakteristieken van boven- en ondergronden in Nederland: de Staringreeks. ⟨https://doi.org/10.18174/512761⟩.

Heinen, M., Brouwer, F., Teuling, C., Walvoort, D.J.J., 2021. BOFEK2020 - Bodemfysische schematisatie van Nederland: update bodemfysische eenhedenkaart. Rapport / Wageningen Environmental Research BT - BOFEK2020 - Bodemfysische schematisatie van Nederland: update bodemfysische eenhedenkaart. ⟨https://doi.org/10.18174/541544⟩.

Levidow, L., Zaccaria, D., Maia, R., Vivas, E., Todorovic, M., Scardigno, A., 2014. Improving water-efficient irrigation: Prospects and difficulties of innovative practices. Agric. Water Manag. 146, 84–94. https://doi.org/10.1016/J.AGWAT.2014.07.012.

Liebhard, Gunther Carl, Klik, A., Stumpp, Christine, Gabriela Morales Santos, Angela, Eitzinger, Josef, Nolz, Reinhard, 2022. Estimation of evaporation and transpiration rates under varying water availability for improving crop management of soybeans using oxygen isotope ratios of pore water. Int. Agrophys. 36, 181–195. https://doi.org/10.31545/intagr/150811.

Mondaca-Duarte, F.D., Heinen, M., van Mourik, S., 2020a. Performance analysis method for model-based irrigation strategies under uncertainty. MethodsX, 101075. https://doi.org/10.1016/j.mex.2020.101075.

Mondaca-Duarte, F.D., van Mourik, S., Balendonck, J., Voogt, W., Heinen, M., van Henten, E.J., 2020b. Irrigation, crop stress and drainage reduction under uncertainty: a scenario study. Agric. Water Manag 230. https://doi.org/10.1016/j.agwat.2019.105990.

Morison, J.I., Baker, N.R., Mullineaux, P.M., Davies, W.J., 2008. Improving water use in crop production. Philos. Trans. R. Soc. Lond. B Biol. Sci. 363, 639–658. https://doi.org/10.1098/rstb.2007.2175.

Perry, C., Steduto, P., Allen, Richard, G., Burt, C.M., 2009. Increasing productivity in irrigated agriculture: Agronomic constraints and hydrological realities. Agric. Water Manag. 96, 1517–1524. https://doi.org/10.1016/j.agwat.2009.05.005.

Sarkar, D., Modak, J.M., 2005. Pareto-optimal solutions for multi-objective optimization of fed-batch bioreactors using nondominated sorting genetic algorithm. Chem. Eng. Sci. 60, 481–492. https://doi.org/10.1016/j.ces.2004.07.130.

Sensoy, S., Ertek, A., Gedik, I., Kucukyumuk, C., 2007. Irrigation frequency and amount affect yield and quality of field-grown melon (Cucumis melo L.). Agric. Water Manag. 88, 269–274. https://doi.org/10.1016/J.AGWAT.2006.10.015.

Turan, A., Ucar, Y., Kazaz, S., 2015. Effects of different irrigation treatments on quality parameters of cut chrysanthemum. Sci. Pap. - Ser. B, Hortic. 419–426.

Udias, A., Pastori, M., Malago, A., Vigiak, O., Nikolaidis, N.P., Bouraoui, F., 2018. Identifying efficient agricultural irrigation strategies in Crete. Sci. Total Environ. 633, 271–284. https://doi.org/10.1016/j.scitotenv.2018.03.152.

van Mourik, S., van der Tol, R., Linker, R., Reyes-Lastiri, D., Kootstra, G., Koerkamp, P. G., van Henten, E.J., 2021. Introductory overview: Systems and control methods for operational management support in agricultural production systems. Environ. Model. Softw. 139, 105031 https://doi.org/10.1016/j.envsoft.2021.105031.

Voogt, W., Kipp, J.A., de Graaf, R., Spaans, L., 2000. A fertigation model for glasshouse crops grown in soil. In: Acta Horticulturae. International Society for Horticultural Science (ISHS). Leuven, Belgium, pp. 495–502. https://doi.org/10.17660/ActaHortic.2000.537.58.

Vrugt, J.A., Stauffer, P.H., Wöhling, T.H., Robinson, B.A., Vesselinov, V.V., 2008. Inverse modeling of subsurface flow and transport properties: a review with new developments. Vadose Zone J. 7, 843–864. https://doi.org/10.2136/vzj2007.0078.

Wang, Yuanji, Liu, L., Wang, Ying, Tao, H., Fan, J., Zhao, Z., Guo, Y., 2019. Effects of soil water stress on fruit yield, quality and their relationship with sugar metabolism in 'Gala' apple. Sci. Hortic. 258, 108753 https://doi.org/10.1016/j.scienta.2019.108753.

Wei, Z., Yoshimura, K., Wang, L., Miralles, D.G., Jasechko, S., Lee, X., 2017. Revisiting the contribution of transpiration to global terrestrial evapotranspiration. Geophys. Res Lett. 44, 2792–2801. https://doi.org/10.1002/2016GL072235.